PHILOSOPHICAL TRANSACTIONS OF THE ROYAL SOCIETY A MATHEMATICAL, PHYSICAL & ENGINEERING SCIENCES

Astronomical calibration of Oligocene--Miocene time

N. J. Shackleton, S. J. Crowhurst, G. P. Weedon and J. Laskar

Phil. Trans. R. Soc. Lond. A 1999 **357**, 1907-1929
doi: 10.1098/rsta.1999.0407

THE ROYAL SOCIETY

Astronomical calibration of Oligocene–Miocene time

By N. J. Shackleton[1], S. J. Crowhurst[1], G. P. Weedon[2] and J. Laskar[3]

[1]*Godwin Laboratory, Department of Earth Sciences, University of Cambridge, Pembroke Street, Cambridge CB2 3SA, UK*
[2]*Department of Environment, Geography and Geology, University of Luton, Park Square, Luton, Bedfordshire LU1 3JU, UK*
[3]*Astronomie et Systemes Dynamiques, Bureau des Longitudes, 77 Av. Denfert-Rochereau, F-75014 Paris, France*

Lithological cyclicity was observed aboard the JOIDES RESOLUTION in sediment sequences recovered from the Ceara Rise during ODP Leg 154. Shipboard work led to the conclusion that the Oligocene was probably characterized by *ca.* 41 ka cycles. Weedon and others were able to confirm this, and created a provisional time-scale for the Oligocene by assuming that the cyclicity is a response to orbital obliquity variation, and by using spectral analysis to estimate the mean wavelength and hence the sedimentation rate of successive intervals of core. We have extended this work by intercorrelating almost all the 9.5 m sediment cores from each of the four sites that recovered Oligocene sediment. We have successfully correlated all the material covering a time-interval of *ca.* 10 Ma from 18 Ma to 28 Ma, as well as most of the sediment from the 14–18 Ma and 28–34 Ma intervals. Although variability is dominated by the 41 ka cycle there is sufficient variability at the precession period (amplitude-modulated by eccentricity) to permit an absolute placement of this section with reference to the calculated orbital history. Further work is needed to establish precisely the implications of this calibration for the geological time-scale but it appears that the true ages of events close to the Oligocene–Miocene boundary are *ca.* 0.9 Ma younger than they appear on recently published time-scales. The sedimentary record preserves information concerning the amplitude modulation of the obliquity signal that is of astronomical as well as geological significance.

Keywords: obliquity, amplitude modulation of; Milankovitch time-scale calibration; Oligocene time-scale; Miocene time-scale; eccentricity, 400 000 year cycle; Ocean Drilling Program, Leg 154

1. Introduction

In this paper we take the data from sedimentary sections that have been assigned approximate ages on the basis of the fossils contained in them, and attempt to refine the age estimates by correlating the sequences to calculated records of variations in the Earth's orbital geometry. In the interval under discussion the biostratigraphic ages that were used are all ultimately linked to the assumed age of the Oligocene–Miocene boundary, for which reason we briefly introduce the basis for this age.

Recent published time-scales for marine sediments of Oligocene and Miocene age (Berggren *et al.* 1985*a*, *b*; Haq *et al.* 1988; Harland *et al.* 1990; Berggren *et al.* 1995)

Table 1. *Location of ODP Leg 154 sites*

hole	latitude	longitude	water depth (m)	depth cored (m)	oldest sediment recovered
925A	4°12.249′ N	43°29.334′ W	3042.2	930.4	Middle Eocene
925C	4°12.256′ N	43°29.349′ W	3040.6	360.1	Early Miocene
925D	4°12.260′ N	43°29.363′ W	3040.5	351.5	Early Miocene
926A	3°43.146′ N	42°54.489′ W	3598.4	327.0	Early Miocene
926B	3°43.148′ N	42°54.507′ W	3598.3	605.8	Early Oligocene
926C	3°43.130′ N	42°54.508′ W	3598.3	398.3	Early Miocene
928A	5°27.320′ N	43°44.884′ W	4010.7	246.7	Early Miocene
928B	5°27.313′ N	43°44.890′ W	4012.2	531.9	Early Oligocene
928C	5°27.315′ N	43°44.906′ W	4012.1	181.5	Middle Miocene
929A	5°58.573′ N	43°44.396′ W	4357.6	527.5	Late Eocene
929E	5°58.568′ N	43°44.402′ W	4356.1	808.9	Late Palaeocene

depend on a complex integration of radiometric age determinations, magnetostratigraphy, and biostratigraphy. We use the terminology for the geomagnetic reversal time-scale (GRTS) of Tauxe *et al*. (1984) and Cande & Kent (1992). It is appropriate to review the basis for ages close to the Oligocene–Miocene boundary. Berggren *et al*. (1985*a*) estimated the age of this portion of the GRTS by assuming that sea-floor spreading in the South Atlantic had proceeded at a constant rate between 10.42 Ma at C5n(o) and 56.14 Ma at C24n(o). Berggren *et al*. (1985*b*) provided evidence that the Oligocene–Miocene boundary falls within C6Cn and gave an age estimate of 23.7 Ma. They did not claim that the boundary could be placed precisely with respect to C6Cn. Cande & Kent (1992, 1995) created a new GRTS; one purpose was to create a time-scale that did not entail imposing artificial instantaneous accelerations in sea-floor spreading at the age control points, so they estimated reversal ages by fitting a cubic spline through a series of distance–age points on a South Atlantic flow line. Cande & Kent (1992, 1995) inserted an age control point at C6C.2n(o), assuming this to represent the Oligocene–Miocene boundary, and assigned an age of 23.8 Ma (from Harland *et al*. 1990). They noted that this figure is close to the boundary age of 23.7 Ma given by Berggren *et al*. (1985*a*) (actually it is even closer to the 23.79 Ma given by Berggren *et al*. (1985*a*) for C6C.2n(o)). This observation is a little misleading, since the figure 23.7 Ma had been derived by assuming a constant spreading rate, but using Late Eocene control points that Cande & Kent (1992) believed were inappropriately old. In the light of the findings of the present paper it is worth remarking that the value of 23.7 Ma given by Berggren *et al*. (1985) would become *ca*. 23.2 Ma if re-estimated with the Eocene–Oligocene boundary at 33.7 Ma (Cande & Kent 1992) instead of by using the age controls that led Berggren *et al*. (1985*a*) to an age of *ca*. 36.5 Ma for the top of the Eocene. The chronogram age that Cande & Kent (1992) used is that given by Harland *et al*. (1990, pp. 155 and 198) where these authors quote an uncertainty of ±1 Ma.

During February and March 1994 the drilling vessel JOIDES RESOLUTION cored five sites over a water-depth transect from 3 to 4.4 km on the Ceara Rise (Curry *et al*. 1995; table 1), recovering *ca*. 5.5 km of sediment. At each site the upper 200 m or so was recovered using the advanced piston corer (APC); at the transition towards

chalk the extended core barrel (XCB) was used; and in fully lithified sediment the rotary core barrel (RCB) was deployed. At each hole in each site successively deeper 9.5 m cores are numbered sequentially, with a suffix H, X or R according to the coring method. The primary objective of this drilling leg was to recover complete sections through the Late Neogene for high-resolution studies, so that at each site several holes were cored with the APC. This strategy enabled the shipboard party to demonstrate that the sedimentary succession at each site had been completely recovered at the scale of the obvious decimetre-scale lithological cyclicity. At four of the sites (925, 926, 928 and 929) coring was extended into the Oligocene, but time did not permit more than one hole at each site to be drilled to the full depth. Thus at each site there may be sediment missing between successive 9.5 m cores.

In the Neogene sections it was relatively easy to demonstrate not only that each site had been completely recovered, but that all of the five sites could be correlated at the scale of each individual lithological cycle (Shipboard Scientific Party 1995, fig. 8). In view of this success, it appeared likely that the same potential for high-resolution intercorrelation existed in older sediments. We have demonstrated that this can be achieved in the Lower Miocene and Upper Oligocene sequences that were recovered.

We do not address here the links between orbitally controlled changes in insolation, climate, ocean circulation, and the quasi-cyclic variations in the character of the sediment. Shackleton & Crowhurst (1997), discussing the Upper Miocene sediments, gave evidence that at least two processes are involved. They argued that variability in the terrigenous input carries a strong precession signal, while sea-floor carbonate dissolution varied with an obliquity-dominated cyclicity. Variability in the productivity of carbonate-secreting organisms in the ocean surface must also make a contribution. Additional work will be needed to determine what factors were dominant during the Oligocene.

2. Material and data

Aboard ship several types of data were gathered that quantitatively document the evident cyclicity.† Whole (unsplit) core sections were analysed on the multi-sensor track (MST) for magnetic susceptibility and natural gamma radiation. The magnetic susceptibility data are presented in volume-normalized SI units; in cases where the core liner was not entirely full, the value is obviously an underestimate but this problem normally only arises while using the RCB to drill hard sediment. Cores from Hole 925A that were undersized were remeasured using a hand-held susceptibility probe to eliminate this uncertainty (Weedon 1997). The gamma ray attenuation porosity evaluator (GRAPE) tool was also in place, but was less useful (because density was relatively constant). The GRAPE does not yield meaningful estimates of sediment density if the recovered sediment does not completely fill the liner, but if the density is estimated independently then it may be possible to use the GRAPE

† The data-sets that form the basis of this paper are very extensive and are only useful in electronic format. The author has made the data available at http://delphi.esc.cam.ac.uk/camdata/wwwcoredata/ODP/rs99index.html and from the ODP database that is in addition a source for the raw data: http://www-odp.tamu.edu/database/. Included and freely available are (i) age models for every core and every downhole log used; (ii) cleaned magnetic susceptibility and reflectance data versus age for each hole; (iii) spliced data-sets used for time-series analysis; and (iv) astronomical data. In addition, the Royal Society maintains an archive copy of the data at http://www.pubs.royalsoc.ac.uk/publish/phi_mpes/rta1757.htm. Subscribers are free to download this data.

data to estimate the diameter of the core. This would provide a means for making a rough correction to the susceptibility and natural gamma estimates which are also affected by incompletely filled core liners, although we have not attempted to do this. After passing through the MST, core sections were split longitudinally and the colour of the cut surface was evaluated using a hand-held spectrophotometer. The output of this device consists of reflectance in 31 successive wavelength bands from 400 to 700 nm; the work presented here was based only on reflectance in the middle of the visible spectrum (550 nm). Finally, in some holes downhole logs were obtained. Generally, these are of little value for the work discussed here, because the resolution of the logging tools is not high enough to retrieve the orbital cyclicity. However, at Site 926 the accumulation rate was quite high, *ca.* 40 m Ma^{-1} in the Oligocene, so that the wavelength of the lithological cycles is of the order of 1.6 m. At this wavelength the cyclicity is well resolved in the downhole spectral gamma ray (SGR) log that integrates the natural gamma emission for the five energy channels that are measured, as well as by the resistivity logs (Shipboard Scientific Party 1995, fig. 16). In addition, parts of the downhole SGR log for Hole 925A are of good quality. The formation microscanner (FMS) was also deployed in Hole 925A; the majority of the record is valueless due to quasi-cyclic loss of contact with the hole walls, but a few intervals of good data were obtained.

To first order all these measurements generate estimates of the proportion of terrigenous material, which is dark-coloured, containing uranium, potassium and iron minerals, relative to biogenic calcium carbonate which is white, non-radioactive and non-magnetizable. The relationships are explored in more detail by the Shipboard Scientific Party (1995, fig. 3) and by Harris *et al.* (1997). Here we note that to use the three data-sets in parallel, it is convenient to scale the shipboard measurements, which have incompatible units, approximately in terms of per cent $CaCO_3$. An alternative strategy would have been to combine all the data and to work with a single per cent $CaCO_3$ record. The reason we have not chosen to do this is that while the three records reflect the same underlying variable, each parameter has its own response characteristics and each data-set is affected by different analytical and diagenetic problems. For example, intervals of very high per cent carbonate are characterized by very high reflectance that is sensitive to small changes, while in contrast the values of the other two parameters are low and within the background noise of the instruments. On the other hand, features in intervals of very low per cent carbonate are better recognized by the exceptionally high magnetic susceptibility, since reflectance is a less sensitive parameter in dark-coloured sediment.

3. Biostratigraphy

The Ceara Rise is geographically well placed for good-quality foraminiferal and nannofossil biostratigraphy, and both groups were well studied by shipboard scientists (Curry *et al.* 1995; Pearson & Chaisson 1997). Unfortunately, the sediments retained no magnetostratigraphic information, due to a pervasive remagnetization induced by the drilling process (Curry *et al.* 1995). Shipboard and post-cruise time-scale work was mainly based on the age assignments in Berggren *et al.* (1995). Siliceous microfossils are very sparsely represented and do not provide useful biostratigraphic information. Unfortunately, there is a paucity of good biostratigraphic datums in the Lower Miocene and Oligocene, and on the basis of published literature it is hard

to evaluate which of them are the most reliable. For this reason the pattern of sedimentation rates for this part of the sedimentary column as reconstructed purely using biostratigraphy is very different from that implied by the sedimentary cyclicity (Weedon *et al*. 1997). Rather than start with a set of biostratigraphic datums that had already been demonstrated by Weedon *et al*. (1997) to be unreliable, the present investigation was built on the preliminary time-scale of these workers.

4. Continuity

A major advantage of having drilled five sites on the Ceara Rise (about the size of the Alps) is that they are close enough to one another to have experienced approximately the same inputs (biogenic and terrigenous) but far enough apart that hiatuses in the various sites are independent. At Site 925 there is a major hiatus with evidence that faulting removed the sediment that had been deposited over the interval 20–24 Ma. At Site 926 faulting has removed the sediment deposited between *ca.* 15 and 17 Ma. Sites 927, 928 and 929 experienced intervals of slumping at times when Site 925 in the shallowest water depth indicates intense carbonate dissolution. Unfortunately, core recovery at Site 925 was inconsistent for sediment from 14 to 18 Ma so that over this interval we were not able to compile a fully complete record, although comparison with the downhole log at Site 925 supports our interpretation of the compilation. Thus we cannot prove on direct geological grounds that there is no hiatus at Site 925 between 15 and 17 Ma. From 18 Ma to almost 30 Ma the resemblance between overlapping segments of data from different sites is excellent and it is unlikely that any significant time is unrepresented.

Some intervals of recovered core contain slumps or turbidites (see Curry *et al*. (1995), pp. 228–230 and table 2 in Weedon *et al*. (1997)). Very thin turbidites have been ignored here; thicker turbidites and slumps have been excised from the records on the assumption that they effectively represent no time and that their deposition did not entail the erosion of any material. For example at 16.091 Ma, *ca.* 3.2 m have been compressed to zero time in both the core and the downhole log at Hole 925A (see figure 1). Some intervals are badly mechanically disturbed by the drilling operation; this applies in particular to the top few decimetres of each core, and where it was evident during visual core description, this is indicated in the 'barrel sheets' (Curry *et al*. 1995, pp. 445–1084). We have excised this material.

5. Orbital data

Laskar *et al*. (1993) made the calculations that, extended for this work, provide the basis for our tuning. It is, however, important to recognize that there are very significant uncertainties in the orbital calculations (see Laskar, this issue) and that our aim was, as far as possible, to achieve a result that is not critically affected by these uncertainties.

The orbital solution is generally considered in two parts: the orbit of the Earth–Moon system around the Sun, and the Earth–Moon interactions that determine the angle and orientation of the Earth's rotational axis. The second of these depends on a knowledge of the physics of the Earth's interior since both tidal friction and departures from the ideal shape for a spinning body affect the results. The changing orbit generates the eccentricity that intervenes in palaeoclimate chiefly through its

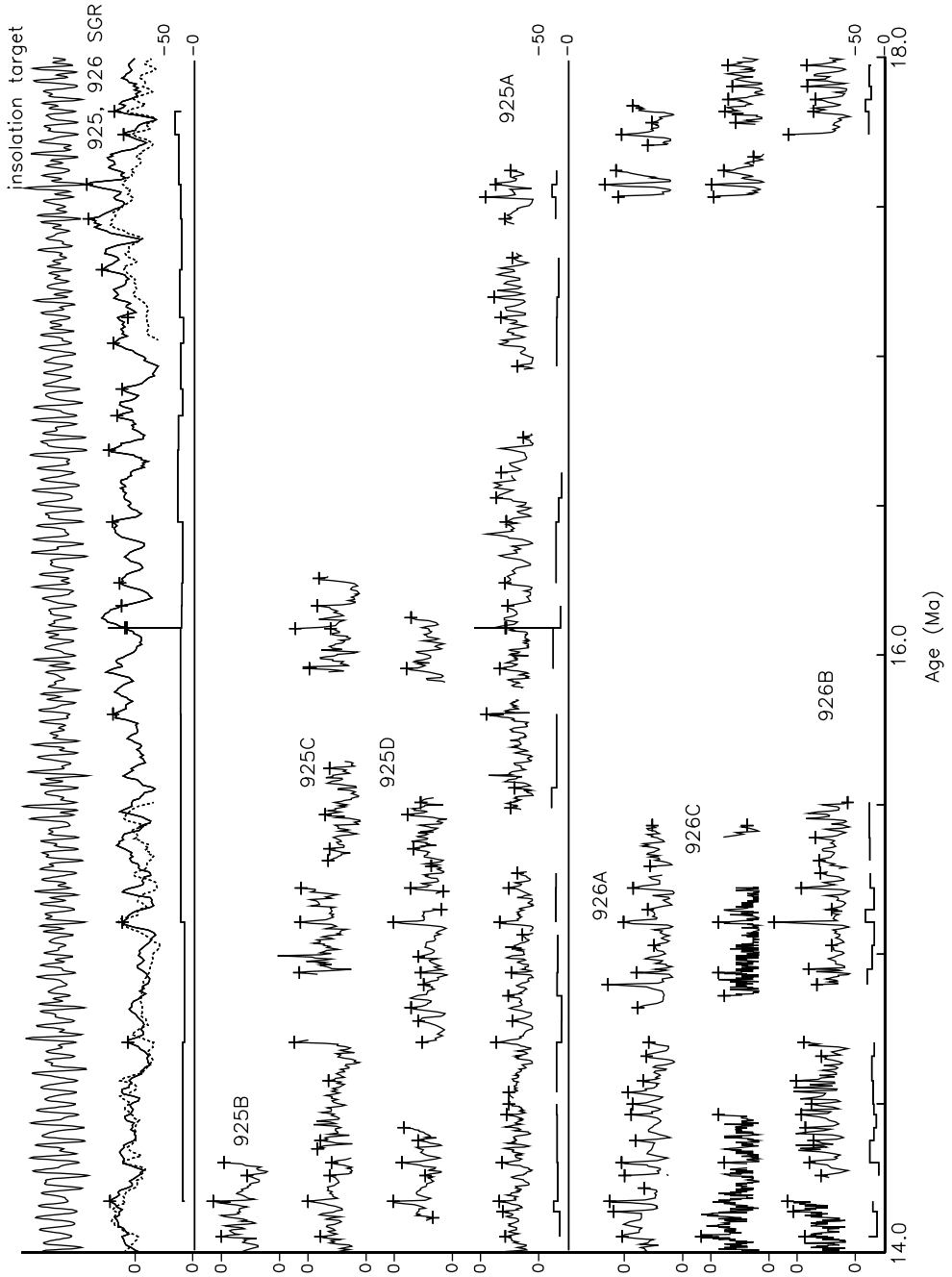

Figure 1. Data for the interval 14–18 Ma. Reading from the top: insolation target; downhole spectral gamma ray logs for ODP Holes 925A (solid) and 926B (dotted, note hiatus); magnetic susceptibility (volume-normalized SI) for Holes 925B, 925C, 925D, 925A, 926A, 926C and 926B. Age control points are marked by crosses; peaks in magnetic susceptibility are tied to minima in insolation. Sedimentation rates for Holes 925A, 926B and 928B and for the 925A downhole log are plotted below the data for these holes (scale m Ma^{-1} on right-hand axis).

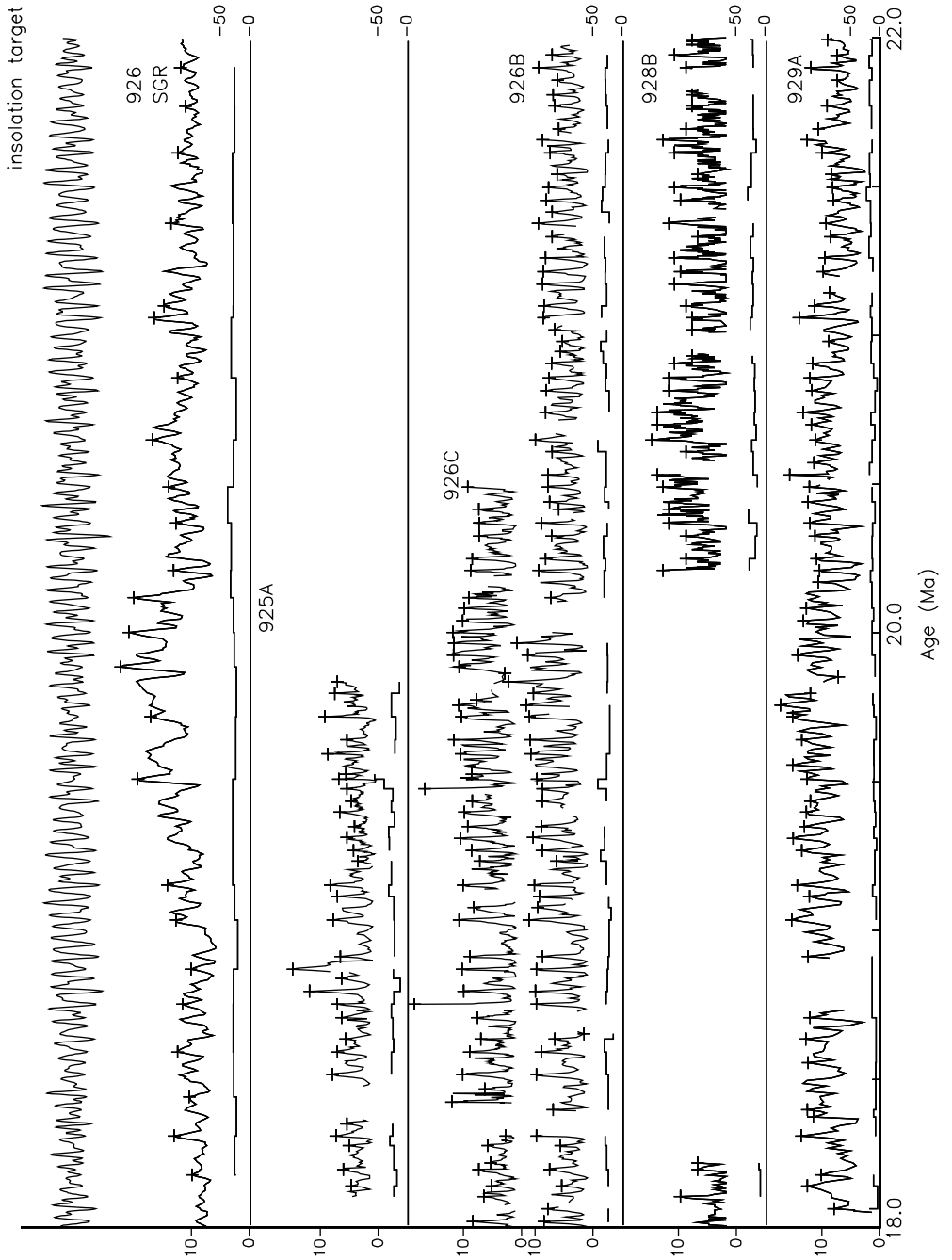

Figure 2. Data for the interval 18–22 Ma. Reading from the top: insolation target; downhole spectral gamma ray log for ODP Hole 926B; magnetic susceptibility (volume-normalized SI) for Holes 925A, 926C, 926B, 928B and 929A. Age control points are marked by crosses; peaks in magnetic susceptibility are tied to minima in insolation. Sedimentation rates for Holes 925A, 926B, 928B and 929A and for the 926B downhole log are plotted below the data for these holes (scale m Ma^{-1} on right-hand axis).

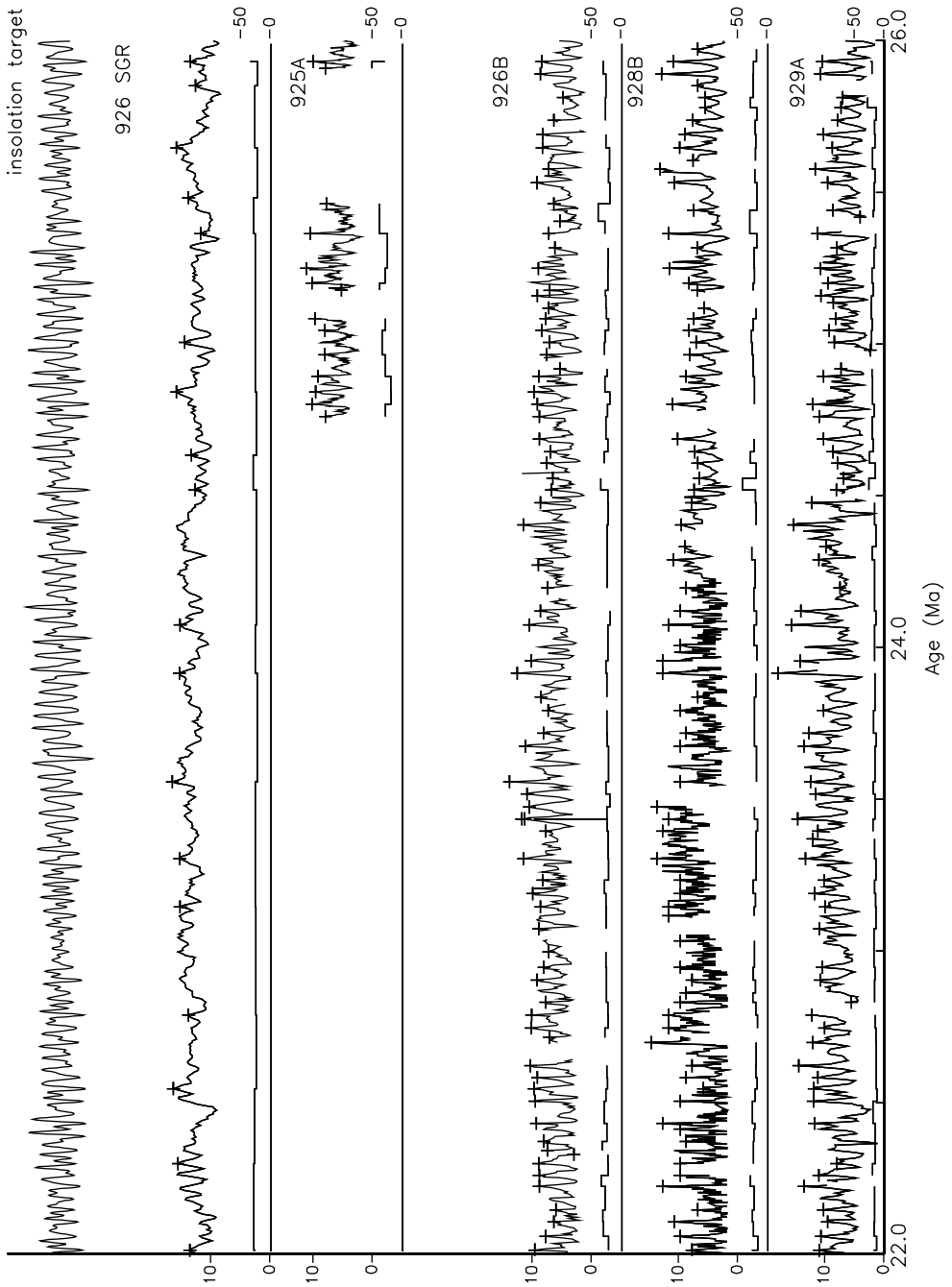

Figure 3. Data for the interval 22–26 Ma. Reading from the top: insolation target; downhole spectral gamma ray log for ODP Hole 926B; magnetic susceptibility (volume-normalized SI) for Holes 925A, 926B, 928B and 929A. Age control points are marked by crosses; peaks in magnetic susceptibility are tied to minima in insolation. Sedimentation rates for Holes 925A, 926B, 928B and 929A and for the 926B downhole log are plotted below the data for these holes (scale m Ma^{-1} on right-hand axis).

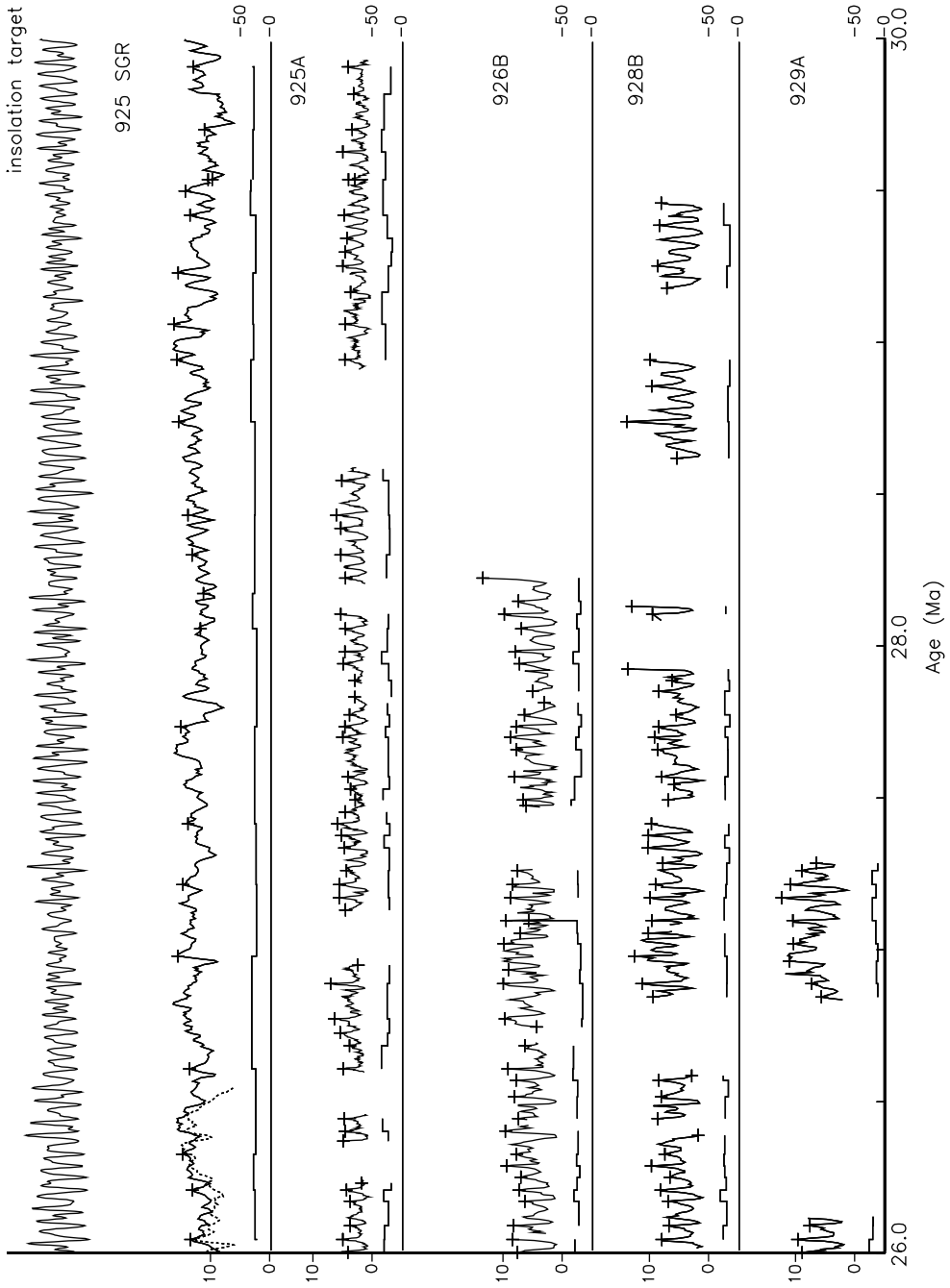

Figure 4. Data for the interval 26–30 Ma. Reading from the top: insolation target; downhole spectral gamma ray log for ODP Hole 925A and (dotted) the bottom of Hole 926B; magnetic susceptibility (volume-normalized SI) for Holes 925A, 926B, 928B and 929A. Age control points are marked by crosses; peaks in magnetic susceptibility are tied to minima in insolation. Sedimentation rates for Holes 925A, 926B, 928B and 929A and for the 925A downhole log are plotted below the data for these holes (scale m Ma^{-1} on right-hand axis).

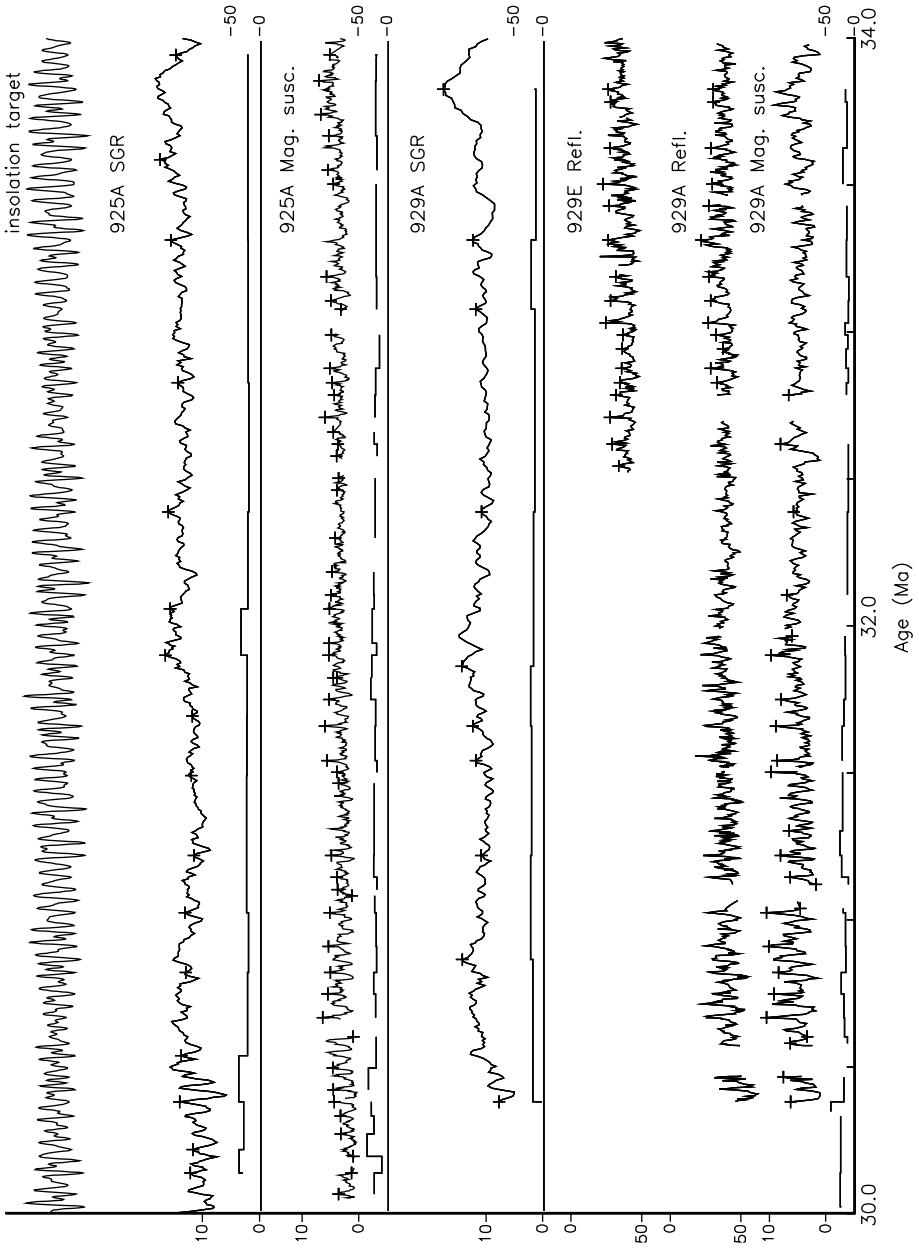

Figure 5. Data for the interval 30–34 Ma. Reading from the top: insolation target; downhole spectral gamma ray log for ODP Hole 925A; magnetic susceptibility for Hole 925A; downhole spectral gamma ray log for Hole 929A; reflectance for Hole 929E; reflectance for Hole 929A and magnetic susceptibility (volume-normalized SI) for Hole 929A. Age control points are marked by crosses; peaks in magnetic susceptibility are tied to minima in insolation, except for the oldest parts of the records from Holes 929A and 929E, where reflectance minima are used for age control points. Note that % reflectance is plotted with reversed scale (0–50). Sedimentation rates for Holes 925A and 929A, and for the 925A and 929A downhole logs, are plotted below the data for these holes (scale m Ma^{-1} on right-hand axis).

modulation of the precession cycle. The frequencies of obliquity and precession both depend on the second set of calculations.

6. Tuning methods

When tuning a Plio-Pleistocene geological record, one is able to assume that the visual pattern of the orbital insolation forcing is known. Consequently, if one examines the history of changing Northern Hemisphere summer insolation through successive obliquity cycles the pattern changes largely as a consequence of the fact that the average precession period is not an exact submultiple of the average obliquity period. If one knows the approximate age of a sequence, one may be able to place it unambiguously (with an age uncertainty of very few thousand years) by pattern-matching. In contrast, by the time we reach the Oligocene the uncertainties in the astronomical calculations mean that the pattern-matching exercise becomes misleading or meaningless. It is then important to clarify the successive procedures through which we have built a geological time-scale based on observed cyclicity.

The first step that we performed was high-resolution correlation between sequences (building on the work of Weedon *et al*. (1997)). In the case of the sites cored during ODP Leg 154, high-precision correlation provides the opportunity to determine changing vertical gradients with respect to water depth in parameters such as per cent $CaCO_3$ or $\delta^{18}O$, permitting reconstructions of the Oligocene water masses to be attempted.

The second step was to identify in the sequences, either individually or in a composite form, the imprint of a particular component of the orbital forcing. In the present study, the obliquity cycle was selected since it dominates the variability in Oligocene sediments. We then made a depth-to-time conversion that matched the sedimentary cycles above and below the base of the Miocene to a sequence of obliquity cycles. Since the ages assigned have an inherent uncertainty of at least ± 1.0 Ma, we could have used a sine wave with 41 ka wavelength instead of a calculated obliquity record. Regardless of the absolute ages that emerge from this exercise, this floating record has the very considerable geological value of permitting sedimentary fluxes and rates of evolutionary change to be evaluated with a resolution and accuracy that is far better than can be achieved by traditional geological means. In addition it may be possible to examine such a floating record that has been aligned to an arbitrary series of obliquity cycles, in order to investigate the response of the system in the precession and obliquity frequency bands, although questions relating to the phase of the response cannot be addressed. It is only after all the sites have been displayed on a common time-scale that the high-resolution site-to-site correlations can be completed. This site-to-site correlation has probably been achieved correctly (to within a few thousand years) for most of the material recovered from the time-interval 18–28 Ma.

Procedurally, the work was done using a workstation for interpolation and statistical analysis. Comparison of and modifications to time-series from different sites were facilitated by using sheets of paper and a light box so that different data-sets could be rapidly overlaid on the basis of an increasingly refined common age scale. Although figures 1–5 only show magnetic susceptibility data, we made equal use of reflectance data and occasional use of natural gamma data, core photographs and downhole logs. We always display implied sedimentation rates between control points in the course of tuning work.

The third step was to examine this 'floating' sequence in the light of the geological uncertainty in its absolute age, and investigate how far it was possible to step down the hierarchy of successively shorter-period orbital cycles and determine precisely which one is represented, and then determine the absolute (astronomical) uncertainty in the age. Weedon *et al*. (1997) chose to fix their time-scale on the assumption that the age of the Oligocene–Miocene boundary is identified with the upper limit of *Sphenolithus delphix* and that this event has an age of 23.8 Ma. We found that in this interval the obliquity signal has a long period variation in amplitude with reduced amplitude cycles very close to the boundary and higher-amplitude cycles above and below. This pattern does not match the calculated obliquity at the accepted age for the boundary; the most likely position is at the amplitude minimum, somewhat younger. Once the whole sequence had been put on a floating age model based on obliquity cycles, it was possible to use amplitude modulation of the precession signal controlled by the long period component of eccentricity (406 ka), and work successively through the *ca.* 100 ka cycle while maintaining the obliquity as the main tuning basis. It should be emphasized that although the long-period amplitude modulations are the key to assigning the correct age to a tuned sequence, the actual tuning can generally only be performed through the clearest cyclicity in the geological records, which is normally either obliquity (as in the present case) or precession cycles.

As mentioned above, the Oligocene and Lower Miocene sediments display a strong 41 ka cyclicity; however, variability with about twice this frequency, presumably attributable to precession, exists in some intervals. For this reason we used as a tuning target a curve that is dominated by obliquity but contains a significant and visible precession component. We chose this approach because the June 65° N curve that is traditionally used as a tuning target is so dominated by the precession component as to be unusable here. On the other hand it is helpful to use a tuning target that contains a precessional component (rather than tuning to pure obliquity) because it assists in aligning core segments with a precessional signal of higher amplitude alongside intervals of high precessional forcing (i.e. periods of high eccentricity). Our tuning target contains four times the proportion of the obliquity component that is present in the mid-June 65° N insolation record and is approximately equivalent to the pattern of varying insolation at 65° N integrated over seven months centred on midsummer. In order to avoid forcing variability into the precession band, we did not insert control points more frequently than one per 41 ka cycle. However, it must be emphasized that any procedure that fixes data extremes to insolation extremes does have the effect of enhancing the coherence with precession. It must also be emphasized that although the tuning target nominally represents the phase for Northern Hemisphere summer, the uncertainties in the orbital calculations are such that this assumption neither affects the result, nor provides a testable hypothesis, at the present time.

7. Results

The age models resulting from our tuning are given in tables 3–14.† Each hole at each site is allocated a separate table. Age is given in million years to three significant decimal places. Depth mbsf (metres below sea floor) is the drilling depth reported

† See footnote on p. 1909.

in primary data (Curry *et al*. 1995). Depth mcd (metres composite depth) is a practically useful but artificial scale which is created so that events observed in two or more holes at the same site are reported at approximately the same depth (see Hagelberg *et al*. 1992). In creating the mcd scale, a fixed depth offset is applied to each 9.5 m core. This scale is extremely useful but has the disadvantage that the scale is usually slightly (*ca*. 10%) stretched with respect to *in situ* depth; there are several reasons for this, including the fact that the sediment does expand in length on recovery and release from overburden pressure (Moran 1997). In a few cases (marked as such) we have modified the mcd scale; in particular adjustments were made for Hole 925A to avoid depth overlap between successive cores. Note that downhole logs were assigned separate age–depth relationships because the position of the logging tool during a logging run is subject to uncertainties that are independent of those relating to the position of the drill bit during core recovery (the depth scales for the published downhole log data have already been processed to remove some of this uncertainty; see Curry *et al*. (1995), p. 34). All depths are given to two decimal places in metres. While this is approximately the precision at which measurement positions are estimated along the core, it must be remembered that the reflectance estimate relates to a 3 mm diameter window of sediment, the magnetic susceptibility is measured using a loop surrounding the core and thus represents over 10 cm of core, and each natural gamma measurement represents the *ca*. 30 cm length of core that is inside the detection chamber during a count. The downhole logging tools integrate the sedimentary record over even greater intervals of 1 m or more (apart from the FMS which has a resolution of only a few centimetres).

The data are shown on our tuned time-scale in figures 1–5. Each figure shows the target orbital curve; the downhole SGR logs for Holes 925A and 926B; magnetic susceptibility for Sites 925, 926, 928 and 929. For each data series the age control points are marked by crosses. Below the data for each site, the implied sedimentation rate between each pair of control points is shown for the primary hole at that site.

These age models are based on the examination of some 10^5 measurements and there are a great many sources of uncertainty, as well as a degree of subjectivity, in the detailed results. We have attempted to create a time-scale for every core recovered, either by matching it to the orbital template or by making a best match to the correlative interval in another site that was more readily tuned to the orbital template.

This operation has already been successfully applied to the interval younger than *ca*. 14 Ma (Shackleton & Crowhurst 1997) and in this work to the interval from *ca*. 18 to 28 Ma. The interval from 14 to 18 Ma is affected by a hiatus (probably the result of slumping as a consequence of intense carbonate dissolution) at Site 926 (Flower *et al*. 1997), and by major slumps at Site 928. The sediments in this interval are exceptionally dissolved, leading to low accumulation rates and loss of stratigraphic resolution, especially in Site 929 which was cored at the deepest water depth. At Site 925 this part of the section was recovered by rotary drilling in Site 925A and suffers from poor recovery and drilling disturbance. Because of these limitations we developed only an outline age model for this interval. However, this suffices to demonstrate that there is no conflict with the ages assigned to sediments older than 18 Ma. The age models that we have developed for the 14–18 Ma interval are tabulated although they should be used with caution; more comprehensive records covering this interval are required to verify the time-scale.

We attempted to deal with the Lower Oligocene in order to address the issue of the duration of the Oligocene; Weedon *et al*. (1997) concluded that the duration of the Early Oligocene may have been significantly greater than indicated by the time-scale of Berggren *et al*. (1995). Fortunately, in this interval the downhole SGR log of Hole 925A is of good quality, and we have been able to construct a plausible age model extending to the Eocene–Oligocene boundary. Again the provisional time-scales are tabulated. As may be seen from the data in table 2, this time-scale brings events close to the Eocene–Oligocene boundary near to the published estimates. Berggren *et al*. (1995) and Prothero (1994) argue that ages in this interval are rather well constrained (in contrast to the situation near the Oligocene–Miocene boundary).

8. Statistical evaluation

Just as there were two phases to the development of this time-scale, so there are two aspects to its evaluation. The first aspect concerns the following questions. 'Are the intervals between events correctly estimated? Are the implied sedimentation rates correct?' The second aspect concerns the question 'are the absolute ages of the events correctly estimated?'

The first question must first be considered from a geological point of view. Through most of the interval investigated here, each site is represented by only a single hole, so that it is only by site-to-site comparisons, together with downhole log data where these have adequate resolution, that the plausibility of our treatment of the inter-core gaps can be tested. Faulting has removed a substantial section that includes the Oligocene–Miocene boundary in Site 925, so that the best record is presented by Site 926. Figures 1–5 show the extent to which the continuity of the record of this site is documented both by comparison with the downhole SGR log, and by comparison with overlapping segments from other sites. It is remarkable how consistently the gradient in implied sedimentation rates as a function of water depth, the result of increasing carbonate dissolution in deeper water, is maintained through time. Implied sedimentation rates generally vary slowly over the 18–30 Ma interval. In the interval from 30 to 34 Ma we have not attempted a detailed tuning, but a modest number of age controls enables the alignment between observed and predicted cyclicity to be maintained. The amplitude of variability is small (in fact the sediments of Early Oligocene age were the most monotonous of all the material recovered during ODP Leg 154).

To evaluate the absolute age of the tuned section we made statistical comparisons with the orbital target. In order to perform statistical analyses of the entire interval, we created a spliced record that is based chiefly on data from Site 926, with *ca.* 10% data from Site 928 and 6% from Site 925 inserted in gaps in the record of Site 926. To create this splice without steps at insertion points, the absolute values for each spliced-in section were multiplied by an adjustment factor so as to minimize their difference relative to the values for Site 926 at the splice points. In order to evaluate the relationship between our tuned record and orbital eccentricity we demodulated the record at a central frequency of 5×10^{-5} cycles per year (figure 6) and carried out a cross-spectral analysis of eccentricity against the amplitude of the demodulated signal (figure 7). A very clear spectral peak with a period of *ca.* 406 ka is strikingly coherent with eccentricity and exactly in phase. This suggests that either our time-

scale is broadly correct, or that it should be shifted by a multiple number of 406 ka cycles.

We also performed complex demodulation of the spliced record, and of calculated obliquity, at a central frequency 2.5×10^{-5} cycles per year. Somewhat to our surprise these two records demonstrate very similar amplitude modulation (figure 6). Cross-spectral analysis shows a prominent spectral peak in both records at a period of *ca.* 1.2×10^6 years. There is no significant phase difference between the amplitude variations in calculated obliquity, and the amplitude modulation in the data. Obliquity is also modulated at a period *ca.* 1.7×10^5 years; in the data this modulation is in the noise level, but nevertheless the signal is (barely) coherent and has zero phase lag. Inspection of the data (figure 6) suggests that the geological data do indeed have the potential to reveal information relating to the history of the obliquity cycle and hence of the controlling periodicities (Laskar, this issue, table 6). We believe that this is the first time that coherence between amplitude modulation in obliquity, and in the response of the climate system to changing obliquity, has been clearly demonstrated, although Lourens & Hilgen (1997) drew attention to the importance of this amplitude modulation, and Maslin *et al.* (1998) suggested a possible palaeoclimatic significance of the increase in obliquity variability between 3.2 and 2.8 Ma. This finding is very significant since the amplitude modulation of obliquity variation does not depend on dynamical ellipticity or tidal friction but only on the $s_3 - s_4$ difference (Laskar, this issue). It is interesting that the spectrum shows a peak in variance at a period close to 406 ka that probably documents a nonlinear interference between response to obliquity and to precession.

The combination of evidence from the amplitude modulation of precession and of obliquity provides good support for our age model with an uncertainty of the order of a fraction of a 406 ka eccentricity cycle; over the interval 18–28 Ma the statistical uncertainty of the estimated phase is as good as $\pm 20°$ (*ca.* ± 20 ka) even when estimated over individual 2 Ma segments. At the '100 ka' period (actually *ca.* 96 ka and 120 ka) the amplitude modulation in the data is not coherent with eccentricity. It should be noted that the spectra are plotted on a linear scale, and demonstrate that the 100 ka signal in amplitude modulation is weaker than is to be expected by comparison with the 406 ka signal. Possibly this could be changed by making more closely spaced measurements on the cores. At the older end of the interval under discussion (*ca.* 27 Ma) the relationships are less elegant; additional work is needed to verify the continuity of the records below this point.

Lourens *et al.* (1996) explored the effect of varying dynamical ellipticity over a range 0.9977–1.002 (taking the present value as 1) and of varying tidal dissipation between zero and the present value, taken as 1, using the calculations of Laskar *et al.* (1993). Their investigations extended to 5.3 Ma and their conclusion was approximately equivalent to stating that mean dynamical ellipticity over this interval was within a factor 1 ± 0.001 of its present value. This uncertainty implies that the age of the 500th obliquity maximum counting back from the present (*ca.* 20 Ma) has an age uncertainty of more than ± 0.1 Ma, or that there is an uncertainty of *ca.* ± 3 in the estimate of the number of obliquity maxima that must be counted back in time to reach a particular orbital eccentricity maximum. Thus the value for dynamical ellipticity must be refined in younger material before we can make the statement that an event at 20 Ma can be associated with a particular obliquity (or precession) cycle. The true age uncertainty in our assignations cannot be better than of the order

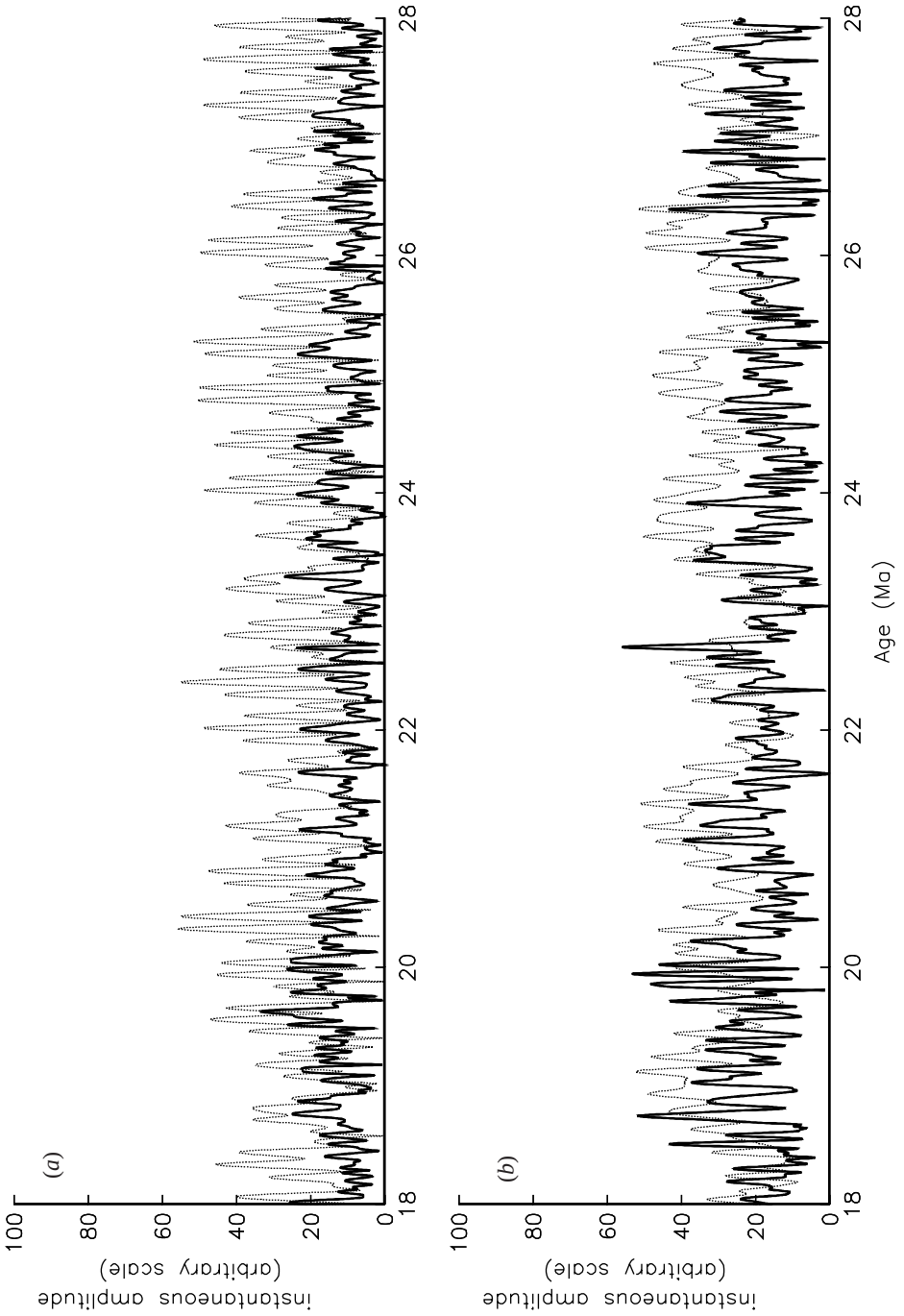

Figure 6. (*a*) Amplitude of the 21 ka variability (obtained by complex demodulation) of a spliced magnetic susceptibility record for the interval 18–28 Ma (solid) compared with orbital eccentricity (dotted) over the same time-interval (Laskar *et al*. 1993). (*b*) Amplitude of the 41 ka variability (obtained by complex demodulation) of the spliced record (solid), compared with amplitude of the obliquity variability (dotted) from Laskar *et al*. (1993).

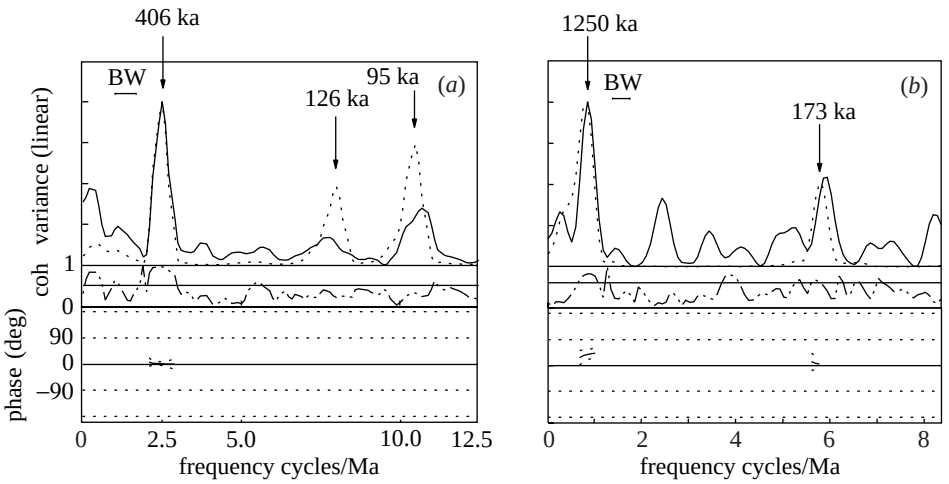

Figure 7. (*a*) Cross-spectral analysis of eccentricity (solid line) versus the amplitude of the 21 ka variability in magnetic susceptibility (dotted line, shown in figure 6). Note high coherency (dash/dotted line) at a period close to 406 ka. (*b*) Cross-spectral analysis of the amplitude of obliquity variability (solid line) versus the amplitude of the 41 ka variability in magnetic susceptibility (dotted line, shown in figure 6). Note high coherency (dash/dotted line) at a period close to 1.25 Ma, and a second peak at a period of *ca.* 170 ka. In both panels the bar labelled BW indicates the bandwidth; phase is only plotted where there is significant coherence and a common peak in variance.

±25 ka. The meaning of this uncertainty estimate is that with good geological material, it should be possible in succession to place events in the correct 1.2 Ma obliquity envelope, and then into the right part of the correct 406 ka eccentricity maximum, and then in the right portion of the correct 100 ka eccentricity maximum. We believe that we have achieved this in the neighbourhood of the Oligocene–Miocene boundary.

9. Biostratigraphic calibrations

Table 2 gives our calculated ages for all biostratigraphic datums given by Curry *et al.* (1995) and by Pearson & Chaisson (1997), together with the published ages as given in these papers. For each datum level we give the calculated ages at the top and bottom of the depth range within which the datum falls. The best estimates are generally derived from whichever site we judge the most reliable and are given to 0.1 Ma except in the case of a few nannofossil datums that have been determined with exceptional precision. A detailed discussion of table 2 is beyond the scope of this paper but several points should be made. First, the material recovered during ODP Leg 154 is far superior to many of the sequences on which previous estimates for the ages of these datums have been based, so that it should come as no surprise that some estimates have been revised quite substantially. Second, it is rarely possible to study such a long sequence in a single composite section; thus the intervals between biostratigraphic events are better constrained than in most publications. Third, it is evident that some biostratigraphic datums are of little value even in these favourable circumstances. Finally, although summary publications (e.g. Berggren *et al.* 1995) provide calibrations of many of these datums to a GRTS, in most cases the magnetostratigraphic data on which the calibrations are

PHILOSOPHICAL TRANSACTIONS OF THE ROYAL SOCIETY A MATHEMATICAL, PHYSICAL & ENGINEERING SCIENCES

Table 2. *Biostratigraphic datums and their ages*

(Unless otherwise noted all ages are based on the depth limits given by Pearson & Chaisson (1997) for foraminifera, and by I. Raffi & J. Backman in Shipboard Scientific Party (1995*b*–*e*) for nannofossils. FO, first occurrence; FCO, first common occurrence; LO, last occurrence; LCO, last common occurrence; AE, acme end.)

biostratigraphic datum	literature age	Site 925 age top	Site 925 age bottom	Site 926 age top	Site 926 age bottom	Site 928 age top	Site 928 age bottom	Site 929 age top	Site 929 age bottom	tuned age
LCO *Cyclicargolithus floridanus*	13.2	13.273	13.333	13.294	13.323	13.214	13.289			13.3
FO *Fohsella fohsi*	13.5	13.394	13.411	13.391	13.451					13.4
LO *Sphenolithus heteromorphus*	13.6	13.541	13.566	13.484	13.534	13.736	13.820			13.55
FO *Fohsella 'praefohsi'*	14.0	14.009	14.078	13.932	13.984	13.453	13.966			14.0
LO *Clavatorells bermudezi*		13.674	14.043	13.984	14.040					13.9
LO *Fohsella periferoronda*	14.6	14.078	14.138	13.984	14.040	13.453	13.966			14.1
LO *Globorotalia archeomenardii*	14.2	14.138	14.201	13.984	14.040					14.2
FO *Fohsella periferoacuta*	14.7	14.136	14.203	14.361	14.432	14.437	14.830			14.3
FO *Globorotalia praemenardii*	14.9	14.280	14.356	14.432	14.512					14.4
LO *Praeorbulina sicana*	14.8	14.431	14.514	14.432	14.512					14.4
LO *Globigerinatella insueta*		14.571	14.652	14.535	14.684	14.437	14.830			14.6
FO *Orbulina universa*	15.1	14.652	14.733	14.685	14.909	14.437	14.830			14.7
FO *Clavatorells bermudezi*		14.829	14.916	14.535	14.684					14.8
LO *Praeorbulina circularis*	14.8			14.535	14.684					14.6
FO *Praeorbulina circularis*	16.0	14.892	14.916	14.685	14.909					14.9
LO *Helicosphaera ampliaperta*	15.8	15.013	15.151	14.909	14.921			15.293	15.559	15.1
FO *Praeorbulina glomerosa*	16.1	16.091	16.280							16.2
FO *Globorotalia archeomenardii*	15.5	16.091	16.280							16.2
AE *Discoaster deflandrei*	16.2	16.057	16.089					15.807	16.077	16.07

PHILOSOPHICAL TRANSACTIONS OF THE ROYAL SOCIETY A MATHEMATICAL, PHYSICAL & ENGINEERING SCIENCES

Table 2. *Cont.*

biostratigraphic datum	literature age	Site 925 age top	Site 925 age bottom	Site 926 age top	Site 926 age bottom	Site 928 age top	Site 928 age bottom	Site 929 age top	Site 929 age bottom	tuned age
FO *Praeorbulina sicana*	16.4	16.954	19.983							17.0
LO *Catapsydrax dissimilis*	17.3	17.476	17.539					17.419	17.636	17.5
FO *Globigerinatella insueta* sstr	18.8	17.539	17.596					17.419	17.636	17.6
FO *Sphenolithus heteromorphus*	18.1			17.666	17.744			17.642	17.709	17.70
LO *Sphenolithus belemnos*	18.4			17.926	17.951			17.806	17.854	17.94
LO *Triquetrorhabdalus carinatus*		18.277	18.315							18.3
LO *Globoquadrina binaiensis*	19.1	18.829	19.055	19.263	19.309			17.919	18.280	18.9
FO *Sphenolithus belemnos*	19.7	18.860	18.876	18.960[a]	18.991[a]	18.689	19.257	18.757	18.948	18.9
FO *Globigerinatella sp.*		19.114	19.216	19.263	19.309			19.144	20.014	19.2
FO *Helicosphaera ampliaperta*				20.324[a]	20.348[a]					20.3
AE *Helicosphaera euphratis*				20.818[a]	20.844[a]					20.8
LO *Paragloborotalia kugleri*	21.6			20.989	21.074	20.164	20.237	20.014	20.198	21.0
LO *Paragloborotalia pseudokugleri*	23.3			21.118	21.321	20.237	21.962	20.014	20.198	21.2
FCO *Helicosphaera carteri*				21.927[a]	21.948[a]					21.9
FO *Sphenolithus disbelemnos*				22.623[a]	22.715[a]			22.669[b]	22.674[b]	22.67
LO *'Globigerina' ciperoensis*				22.783	22.845	22.837	22.967	22.956	23.126	22.8
FO *Globigerinoides trilobus* s.l.				22.845	22.907	22.837	22.967			22.9
FO *Paragloborotalia kugleri*	23.7			22.839	22.903	23.033	23.052	22.956	23.037	22.9
LO *Sphenolithus delphix*	23.7			22.969[a]	23.004[a]	22.952[b]	22.988[b]	22.978[b]	22.983[b]	22.98

*Hole 927A, [a]E. Fornaciari, personal communication (1997), [b]Raffi, this issue.

PHILOSOPHICAL TRANSACTIONS OF THE ROYAL SOCIETY A MATHEMATICAL, PHYSICAL & ENGINEERING SCIENCES

Table 2. *Cont.*

biostratigraphic datum	literature age	Site 925 age top	Site 925 age bottom	Site 926 age top	Site 926 age bottom	Site 928 age top	Site 928 age bottom	Site 929 age top	Site 929 age bottom	tuned age
FO *Sphenolithus delphix*	24.4			23.279[a]	23.310[a]	23.061[b]	23.110[b]	23.234[b]	23.241[b]	23.24
LO *'Globigerina' angulisuturalis*	23.3			23.757	23.906	24.563	24.611	24.610	24.746	23.8
LO *Sphenolithus ciperoensis*	24.7			24.162	24.212	24.114	24.149	24.138[b]	24.143[b]	24.14
FO *Paragloborotalia pseudokugleri*	25.9	24.546	24.590	24.525	24.662	24.611	24.677	24.747	25.070	24.6
LO *Sphenolithus distensus*	26.5	26.271	26.283	26.709	27.096	26.425	26.447	26.341	27.403	26.3
LO *Paragloborotalia opima*	27.1	26.328	26.617	25.270	25.385	25.834	25.960			
FO *Sphenolithus ciperoensis*	28.1	26.901	26.938	26.709	27.096	26.948	26.981	27.403	30.085	26.9
LO *Chiloguembelina cubensis*	28.5	26.941	27.134	27.015	27.069	27.053	27.072	26.990	27.087	27.0
FO *'Globigerina' angulisuturalis*	29.7	29.081	29.169			28.958	29.118	25.157	30.736	29.1
LO *Turborotalia ampliapertura*	30.3	29.169	29.363					30.683	30.736	29.3
FO *Sphenolithus distensus*	30.4	29.354	29.434					31.144	31.513	29.4?
FO *Paragloborotalia opima*	30.6	29.563	29.589					25.682	26.073	29.6
LO $>14\,\mu$m *Reticulofenestra umbilicus*	32.1	32.299	32.357					32.400	32.460	32.3
LO *Coccolithus formosus*	32.7	32.960	33.071					33.123	33.204	33.0
LO *Pseudohastigerina naguewichiensis*	32.5	31.765	31.987							31.9
LO *Hantkeneina alabamensis*	33.75	33.978	34.002					33.754	33.938	33.9
LO *Turborotalia cerroazulensis*	33.9	34.002	34.019					33.938	35.316	34.0
LO *Cribohantkeneina inflata*	34.0	34.085	34.108							34.1
LO *Discoaster saipanensis*	34.4	34.413	34.426					34.786	34.808	34.4

*Hole 927A, [a]E. Fornaciari, personal communication (1997), [b]Raffi, this issue.

based do not bear scrutiny. Raffi (this issue) has re-evaluated the biostratigraphic datums that are close to the Oligocene–Miocene boundary in a site with excellent magnetostratigraphic control. Comparing our ages with the ages for the same events calibrated against the CK95 time-scale suggests that the age calibration point of 23.8 Ma in CK95 for the Oligocene–Miocene boundary should be revised younger by *ca.* 0.9 Ma and the palaeomagnetic time-scale re-calibrated accordingly. Additional work will be required if we wish to use our time-scale in order to insert additional age calibration points into the palaeomagnetic time-scale; in particular, high-resolution biostratigraphic work in the Oligocene is warranted now that a high-resolution time-framework exists.

10. Conclusions

A combination of the data provided here with those of Tiedemann & Franz (1997), and of Shackleton & Crowhurst (1997) provides an unprecedented 30 Ma astronomically tuned sedimentary sequence (with tentative tuning to 34 Ma) in the tropical Atlantic. The Miocene–Oligocene boundary has an age *ca.* 0.9 Ma younger than is generally accepted. As has already been demonstrated by Zachos *et al.* (1997, and unpublished work), this material provides the opportunity to study the Oligocene climate with the resolution that is normally devoted to the Quaternary. Doubtless more surprises will emerge as this opportunity is exploited.

N.J.S. is extremely grateful to his co-chief scientist Bill Curry and the wonderful team of scientists, technicians, drillers and other staff who made ODP Leg 154 such a success, as well as to the ODP scientific planning structure that enabled this drilling to be carried out. We thank Hilary Paul and Jim Zachos for sharing stable isotope data from ODP Site 929 with us. Discussions with Marie-France Loutre and Heiko Pälike clarified our understanding of the real age uncertainties and how they may be reduced, and enhanced our computing skills. The clarity of the manuscript benefited considerably from reviews by Steve Clemens and Nick McCave. This work was supported by the NERC through grants GST/02/971 and GR3/11461 to N.J.S.

References

Berggren, W. A., Kent, D. V. & Van Couvering, J. A. 1985*a* The Neogene. Part 2. Neogene geochronology and chronostratigraphy. In *The chronology of the geological record* (ed. N. J. Snelling). Geological Society Memoir 10, pp. 211–260.

Berggren, W. A., Kent, D. V. & Flynn, J. J. 1985*b* Jurassic to Paleogene. Part 2. Paleogene geochronology and chronostratigraphy. In *The chronology of the geological record* (ed. N. J. Snelling). Geological Society Memoir 10, pp. 141–195.

Berggren, W. A., Kent, D. V., Swisher III, C. C. & Aubry, M.-P. 1995 A revised Cenozoic geochronology and chronostratigraphy. In *Geochronology time scales and global stratigraphic correlation* (ed. W. A. Berggren, D. V. Kent, M.-P. Aubry & J. Hardenbol). *SEPM* (Spec. Publ.) **54**, 129–212.

Cande, S. C. & Kent, D. V. 1992 A new geomagnetic polarity time scale for the Late Cretaceous and Cenozoic. *J. Geophys. Res.* **97**, 13 917–13 951.

Cande, S. C. & Kent, D. V. 1995 Revised calibration of the geomagnetic polarity time scale for the Late Cretaceous and Cenozoic. *J. Geophys. Res.* **100**, 6093–6095.

Curry, W. B. (and 26 others) 1995 *Proc. ODP, Initial Rep.*, vol. 154. College Station, TX: Ocean Drilling Program.

Flower, B. P., Zachos, J. C. & Martin, E. 1997 Latest Oligocene through early Miocene isotopic stratigraphy and deep-water Paleoceanography of the Western Equatorial Atlantic: Sites 926 and 929. In *Proc. ODP, Sci. Results*, vol. 154 (ed. N. J. Shackleton, W. B. Curry, C. Richter & T. J. Bralower), pp. 433–439. College Station, TX: Ocean Drilling Program.

Hagelberg, T., Shackleton, N. J., Pisias, N., & Shipboard Party 1992 Development of composite depth sections for Sites 844 through 854. In *Proc. ODP, Initial Results*, vol. 138 (ed. L. Mayer and 30 others), pp. 79–85. College Station, TX: Ocean Drilling Program.

Haq, B. U., Hardenbol, J. & Vail, P. R. 1988 Mesozoic and Cenozoic chronostratigraphy and cycles of sea-level change. Sea-level changes—an integrated approach. *SEPM* (Spec. Publ.) **42**, 71–108.

Harland, W. B., Armstrong, R. L., Cox, A. V., Craig, L. E., Smith, A. G. & Smith, D. G. 1990 *A geologic time scale 1989*. Cambridge University Press.

Harris, S. E., Mix, A. C. & King, T. 1997 Biogenic and terrigenous sedimentation at Ceara Rise, Western Tropical Atlantic supports Pliocene–Pleistocene deep-water linkage between hemispheres. In *Proc. ODP, Sci. Results*, vol. 154 (ed. N. J. Shackleton, W. B. Curry, C. Richter & T. J. Bralower), pp. 331–345. College Station, TX: Ocean Drilling Program.

Laskar, J., Joutel, F. & Boudin, F. 1993 Orbital, precessional, and insolation quantities for the Earth from −20 Myr to +10 Myr. *Astron. Astrophys.* **270**, 522–533.

Leg 154 Scientific Party (Curry, Shackleton, Richter *et al.*) 1995 Leg 154 Synthesis. In *Proc. ODP, Initial Results*, vol. 154 (ed. W. B. Curry and 26 others), pp. 421–442. College Station, TX: Ocean Drilling Program.

Lourens, L. J. & Hilgen, F. J. 1997. Long-period variations in the Earth's obliquity and their relation to third-order eustatic cycles and late Neogene glaciations. *Quat. Int.* **40**, 43–52.

Lourens, L. J., Hilgen, F. J., Raffi, I. & Vergnaud-Grazzini, C. 1996 Early Pleistocene chronology of the Vrica section (Calabria, Italy). *Paleoceanography* **11**, 797–812.

Maslin, M. A., Li, X. S., Loutre, M.-F. & Berger, A. 1998 The contribution of orbital forcing to the progressive intensification of Northern Hemisphere glaciation. *Quat. Sci. Rev.* **17**, 411–426.

Moran, K. 1997 Elastic property corrections applied to Leg 154 sediment, Ceara Rise. In *Proc. ODP, Sci. Results*, vol. 154 (ed. N. J. Shackleton, W. B. Curry, C. Richter & T. J. Bralower), pp. 151–155. College Station, TX: Ocean Drilling Program.

Pearson, P. N. & Chaisson, W. P. 1997 Late Paleocene to middle Miocene planktonic foraminifer biostratigraphy of the Ceara Rise. In *Proc. ODP, Sci. Results*, vol. 154 (ed. N. J. Shackleton, W. B. Curry, C. Richter & T. J. Bralower), pp. 33–68. College Station, TX: Ocean Drilling Program.

Prothero, D. R. 1994 *The Eocene–Oligocene transition: Paradise Lost* (ed. D. J. Bottjer & R. K. Bambach). Critical Moments in Paleobiology and Earth History Series. Columbia University Press.

Shackleton, N. J. & Crowhurst, S. 1997 Sediment fluxes based on an orbitally tuned time scale 5 Ma to 14 Ma, Site 926. In *Proc. ODP, Sci. Results*, vol. 154 (ed. N. J. Shackleton, W. B. Curry, C. Richter & T. J. Bralower), pp. 69–82. College Station, TX: Ocean Drilling Program.

Shipboard Scientific Party 1995. Leg 154 Synthesis. In *Proc. ODP, Sci. Results*, vol. 154 (ed. N. J. Shackleton, W. B. Curry, C. Richter & T. J. Bralower), pp. 421–442. College Station, TX: Ocean Drilling Program.

Steininger, F. F. (and 14 others) 1997 Proposal for the global stratotype section and point (GSSP) for the base of the Neogene (the Palaeogene/Neogene boundary). In *Miocene stratigraphy: an integrated approach* (ed. A. Montanari, G. S. Odin & R. Coccioni), pp. 125–147. Elsevier.

Tauxe, L., Tucker, P., Petersen, N. P. & LaBrecque, J. L. 1984 Magnetostratigraphy of Leg 73 sediments. In *Initial Rep. DSDP*, vol. 73 (ed. K. J. Hsü and 13 others), pp. 609–621. Washington, DC: US Government Printing Office.

Tiedemann, R. & Franz, S. O. 1997 Deep-water circulation, chemistry, and terrigenous sediment supply in the equatorial Atlantic during the Pliocene, 3.3–2.6 Ma and 5–4.5 Ma. In *Proc. ODP, Sci. Results* (ed. N. J. Shackleton, W. B. Curry, C. Richter & T. J. Bralower), vol. 154, pp. 299–318. College Station, TX: Ocean Drilling Program.

Weedon, G. P. 1997 Data report: measurements of magnetic susceptibility for the Oligocene and Lower Miocene of Site 925. In *Proc. ODP, Sci. Results* (ed. N. J. Shackleton, W. B. Curry, C. Richter & T. J. Bralower), vol. 154, pp. 529–532. College Station, TX: Ocean Drilling Program.

Weedon, G. P., Shackleton, N. J. & Pearson, P. N. 1997 The Oligocene time scale and cyclostratigraphy on the Ceara Rise, Western Equatorial Atlantic. In *Proc. ODP, Sci. Results* (ed. N. J. Shackleton, W. B. Curry, C. Richter & T. J. Bralower), vol. 154, pp. 101–114. College Station, TX: Ocean Drilling Program.

Zachos, J. C., Flower, B. P. & Paul, H. 1997 Orbitally paced climate oscillations across the Oligocene/Miocene boundary. *Nature* **388**, 567–570.

PHILOSOPHICAL TRANSACTIONS OF THE ROYAL SOCIETY A MATHEMATICAL, PHYSICAL & ENGINEERING SCIENCES

PHILOSOPHICAL TRANSACTIONS OF THE ROYAL SOCIETY A MATHEMATICAL, PHYSICAL & ENGINEERING SCIENCES